A Bim-Based Evacuation Assessment of Complex Rail Transit Stations under Post-earthquake Fires for Sustainable Buildings

Hui Xu , Yuxi Wei , Yongtao Tan * , Qilin Zhou

Posted Date: 5 January 2024

doi: 10.20944/preprints202401.0478.v1

Keywords: Evacuation assessment; Post-earthquake fire; BIM; Complex rail transit station; Sustainable buildings

Article

A BIM-Based Evacuation Assessment of Complex Rail Transit Stations under Post-Earthquake Fires for Sustainable Buildings

Hui Xu [1,2], Yuxi Wei [1], Yongtao Tan [3,*] and Qilin Zhou [4]

[1] School of Economics and Management, Chongqing University of Posts and Telecommunications, Chongqing 400065, China; xuhui@cqupt.edu.cn (H.X.); weiyuxi23@163.com (Y.W.)
[2] Chongqing Innovation Center of Industrial Big-Data Co. Ltd., National Engineering Laboratory for Industrial Big-Data Application Technology, Chongqing 400707, China
[3] School of Engineering, RMIT University, Melbourne, VIC 3001, Australia; yongtao.tan@rmit.edu.au(Y.T.)
[4] Chongqing Major Projects Service, Chongqing 401120, China; qilindd@163.com(Q.Z.)
* Correspondence: yongtao.tan@rmit.edu.au

Abstract: Post-earthquake fire is considered as a catastrophic secondary disaster to personal and property safety. In this article, an evacuation assessment of a complex rail transit station under the post-earthquake fire for sustainable buildings was conducted from the internal environment and external rescue based on Building Information Modeling (BIM) and Fire Dynamic Simulation (FDS). The internal environment evacuation assessment simulation experiments were conducted in six hypothetical high-risk scenarios. Besides, the external rescue assessment was based on investigation of the route and the rescue time required during different periods of holidays and workdays. The results show that: (1) The influence caused by different size of fire area in the power distribution room is smaller than those in the train at the platform floor. (2) In the case of fire scenarios with the same fire area but different fire locations, the impact on temperature is greater than that on CO concentration in power distribution room. (3) It shows slight differences between single-floor fire and double-floor fire on evacuation of small area fire in power distribution room. Meanwhile, optimized design recommendations are proposed to reduce the risk of emergency evacuation in both internal and external environments of rail transit stations for sustainable future buildings.

Keywords: evacuation assessment; post-earthquake fire; BIM; complex rail transit station; sustainable buildings

1. Introduction

Earthquakes are recognized as one of the most powerful and impactful natural disasters[1]. According to the statistics of the China Earthquake Networks, 12 *Ms* 8.0 earthquakes occurred around the world from 2012 to 2022, resulting in lots of casualties and economic losses[2]. In addition to direct losses, numerous secondary disasters after an earthquake, such as post-earthquake fire, also cause serious destructive consequences, including people injured, infrastructure damage, etc.[3] The post-earthquake fires can be ignited due to various factors, such as broken gas pipes, open-flame sources, electrical short-circuits, leakage of flammable liquids, etc.[4] Post-earthquake fires have been historically frequent, and each occurrence has resulted in catastrophic damage to the cities and buildings. For instance, on January 17, 1994, the *Mw* 6.7 Northridge earthquake in California caused ground cracks and approximately 110 fires directly attributed to its effects[5]. The Japan Kobe *Ms* 7.3 earthquake caused 269 fires due to natural gas leaking and 7,036 buildings were destroyed in the post-earthquake fires in 1995[6]. A *Mw* 7.8 and *Mw* 7.5 earthquake struck Turkey on February 6, 2023, killing approximately 50,000 people. At the Port of Iskenderun, the earthquake caused a collapse of a part of containers, resulting in a fire that severely impacted port operations. Post-earthquake fires can cause serious harm to buildings, so it is essential to conduct evacuation assessments for providing sustainable improvements to buildings.

 doi:10.20944/preprints202401.0478.v1

Nowadays, complex public spaces with multi-layer structures and high population density, such as rail transit stations, integrated railway transportation hubs, and airport terminals, have become increasingly prevalent[7]. The complex rail transit station facilitates people's transportation and meets the needs of various commercial functions[8]. However, the complex structure, high population density on each floor, and the open nature of these spaces, pose significant challenge for evacuation in the post-earthquake fire[9]. According to statistics of the Ministry of Emergency Management of China's Fire and Rescue Department, electrical fires have increased by 42.7% in the past 10 years[10]. Short circuit, poor electrical contacts, aging electrical equipment and overload are the main causes of electrical fires[11]. Due to lots of circuits and electrical equipment, complex urban public spaces are vulnerable to post-earthquake fires[9]. Emergency evacuation in complex urban public spaces, especially complex rail transit stations, has become a hot topic in recent years. Feng et al.[12] used computational fluid dynamics (CFD) and Agent-based simulation methods to analyze the emergency evacuation capability of a subway transfer station in Guangzhou. Chen et al.[13] numerically simulated the crowd dynamics during the fire evacuation of Xiamen Metro Haicang Avenue station. Xu et al. [14] proposed a method to determine effective emergency evacuation strategies in complex urban public spaces and established an emergency evacuation theoretical framework by using the AnyLogic. Many studies have explored fire simulation in rail transit stations, but few have considered evacuation assessment in complex rail transit stations during post-earthquake fires. Post-earthquake fire rescue is usually more difficult than normal fire because the potential damage. Therefore, conducting evacuation assessments in post-earthquake fires is crucial for providing sustainable improvements to rail transit stations.

Accordingly, this research focuses on the evacuation assessment within the internal environment and external rescue of a complex rail transit station under the post-earthquake fire for sustainable. This research aims to (1) establish a fire simulation model based on BIM and Fire Dynamic Simulation (FDS) application, (2) conduct a case demonstration to verify the feasibility of the established model and assess the evacuation ability of the complex rail transit station, and (3) supply optimization design suggestions for the internal and external environment of the rail transit station to reduce risks in emergency evacuation.

2. Literature review

Several methods have been adopted in post-earthquake fire research. Juliá et al.[15] used the risk matrix to identify fire-prone buildings after the earthquake and 33% of the surveyed buildings were recognized as having a high risk of post-earthquake fire. Based on BIM and virtual reality (VR), Lu et al.[16] explored a simulation framework of indoor post-earthquake fire rescue scene, and a smoke visualization method based on the combination of drawing and particle system was proposed. Risco et al.[4] employed finite element numerical analyses in post-earthquake fire research, which focused on a 5-story structure and a 10-story structure by assuming fire proof components and the absence of heat insulation components. Xu et al.[17] proposed a comprehensive method for the seismic damage assessment of sprinkler systems based on the combination of BIM, computational fluid dynamics (CFD) model, and fire dynamics simulator (FDS) program. According to the existing studies, BIM has been widely employed in post-earthquake fire simulation research. To analyze the virtual fire scenario, a more intuitive model could be built in BIM, allowing for the adjustment of various parameters.

According to existing studies, the following three research gaps can be concluded:

(1) Although numerous studies have been conducted on fire simulation and emergency evacuation in rail transit stations, there is a research gap when it comes to evaluating evacuations under a post-earthquake fire to propose sustainable buildings recommendations.

(2) Currently, little attention given to fire simulations of complex rail transit stations. Complex rail transit stations are characterized by the convergence of multiple lines, intricate spatial structures, and large traffic flow. It is crucial to conduct comprehensive research for complex rail transit stations to develop more effective and sustainable evacuation plans and feasible response measures for post-earthquake fires.

Preprints (www.preprints.org) | NOT PEER-REVIEWED | Posted: 5 January 2024 doi:10.20944/preprints202401.0478.v1

(3) The majority of existing researches are directed towards fire evacuation planning, leaving a significant research gap in assessing the evacuation capacities of sustainable rail transit stations.

3. Methodology

The research methodology consists of five modules: 1) Building Information Modeling (BIM), 2) Fire Dynamic Simulation (FDS), 3) assumptions in Revit and Pyrosim, 4) fire scenarios, and 5) fire simulation.

3.1. BIM

BIM it is an important technology in the construction digitalization world, which can be used by adopting computer visualization technology and simulation method[18]. Based on BIM, buildings can be simulated by BIM to provide valuable management suggestions for subsequent operation and maintenance measures, such as emergency evacuation simulation in earthquake, fire, etc.[19]. It is crucial to gather information about the geometric characteristics of buildings for fire simulation and assessment. This includes accurately representing the following components:

(1) Building structure, such as platform floors, concourse floors, entrances/exits, stairs, elevators, fire-resistant, as well as their quantity, dimensions, height, geometric shapes, position and orientation. This level of detail was particularly crucial for complex structures like a complex rail transit station.

(2) BIM elements association. The relationships between different elements, such as the connection between the platform floor and stairs, elevators, and entrances/exits, should be considered in BIM elements association.

(3) Ventilation and fire protection system. Determine the positioning and layout of ventilation and fire protection systems to ensure the safety of the railway transit station during fires. This involves factors such as smoke control devices, fire-extinguishing systems, fire doors, etc.

Generally, non-graphical information is not required to be included in fire scenarios.

3.2. FDS

3.2.1. FDS model theoretical foundation

The stage of fire development involves a complex dynamic field generated by the interaction of coupled physical and chemical reactions, hydrodynamics, and heat transfer. It mainly follows the conservation equations, which are shown in equations (1)-(4).

(1) Mass conservation law：

$$\frac{\partial \rho}{\partial t} + \nabla \cdot \rho \vec{u} = 0 \tag{1}$$

Where ρ is the density of the combustion gas, t is the combustion time, ∇ is the divergence magnitude, and $\vec{u}$ is the smoke gas velocity.

(2) Energy conservation law：

$$\frac{\partial}{\partial t}(\rho h) + \nabla \cdot (\rho h \vec{u}) = \frac{\partial p}{\partial t} + \vec{u} \cdot \nabla p - \nabla \vec{q}_r + \nabla \cdot (k \nabla T) + \sum_i \nabla (h_i \rho D_i \nabla Y_i) \tag{2}$$

Where h is the enthalpy, P is the ambient pressure, $\nabla \vec{q}_r$ is the radiative heat flux, k is the thermal conductivity, T is the temperature, D is the diffusion coefficient, and Y is the component mass fraction.

(3) Momentum conservation law：

$$\rho(\frac{\partial \vec{u}}{\partial t} + \frac{1}{2}\nabla |\vec{u}|^2) + \nabla p - \rho g = \vec{f}_b + \nabla \cdot \tau_{i_j} \tag{3}$$

Preprints (www.preprints.org) | NOT PEER-REVIEWED | Posted: 5 January 2024 doi:10.20944/preprints202401.0478.v1

Where $\vec{f}_b$ is the external force vector, and τ_{ij} is the viscous stress tensor.

(4) Gas component conservation law：

$$\frac{\partial}{\partial t}(\rho Y_i) + \nabla \cdot (\rho Y_i \vec{u}) = \nabla(\rho D_i \nabla Y_i) + \dot{m}_i^{m} \tag{4}$$

Where $\dot{m}_i^{m}$ is the formation rate.

3.2.2. Pyrosim simulation software introduction

The Pyrosim software, developed by the American Institute of Standard Technology based on FDS, enables fire dynamic simulation. According to the fluid dynamics, the smoke movement, CO concentration and temperature can be predicted under the situation of fire[20]. Based on the conservation equations, the simulation is carried out. After the simulation, the plot time history results of the thermocouples and CO concentration can be viewed in Pyrosim. In addition, the entire fire development stages and smoke spread process can be observed in 3D using Smokeview.

3.3. Assumptions in Revit and Pyrosim

It is assumed that the building structures suffer no considerable damage and the escape routes are not disrupted after the earthquake, at least for the first minutes of the a fire event[21]. In addition, the worst-case scenarios of non-structural damage such as elevator or fire-extinguishing system damage are considered. Besides, people evacuate rooms without closing fire-resistant doors, and non-fire-resistant doors are excluded from the model to focus on simulating critical fire and smoke emissions.

3.4. Fire scenarios

The different locations of fire points in the complex rail transit station have different impacts on emergency evacuation. In order to better respond to emergencies and achieve sustainable future buildings, the most unfavorable principle should be applied in the fire site design. Combustible materials in rail transit station include various components, such as the trains bodies and some circuits[11]. Therefore, this paper mainly considers the locations that are most susceptible to fires: the train and the power distribution room. The specific hypothetical ignition points are illustrated in the case study section.

3.5. Fire scenarios

The fire simulation is divided into the internal environment evacuation simulation and the external environment rescue simulation.

3.5.1. Internal evacuation environment simulation

The standard atmospheric pressure is 101325Pa and the relative humidity before the disaster was 50% without considering the influence of internal wind speed. To improve the detection of the temperature and CO concentration in the populated rail transit station after an earthquake, thermocouples and gas-phase devices are set at the populated area. According to Report on the Nutrition and Chronic Disease Status of Chinese Residents(2020), the average height of a male adult is stated to be 170.6cm and for adult females is 158.7cm[22]. Considering that the height of the human mouth and nose is lower than the height, the height of the thermocouple and gas-phase device are set lower than 170.6cm on each floor. The two important parameters to consider are temperature and CO concentration.

(1) Temperature

Human endurance to high temperatures is limited, particularly when it can cause irreversible damage to the skin and respiratory tract. To ensure the safety of the evacuees, the temperature must be maintained within a certain range. Research reveals that thermal burns to the respiratory tract can

 doi:10.20944/preprints202401.0478.v1

occur when individuals inhale air above 60°C saturated with water vapor[23]. Table 1 shows the maximum exposure time of people at different temperatures. In this research, 60℃ is considered as a threshold value.

Table 1. The maximum exposure time of people at different temperatures.

Exposure Temperature(℃)	Maximum Exposure Time(min)
80	3.8
75	4.7
70	6.0
65	7.7
60	10.1
55	13.6
50	18.8
45	26.9
40	40.2

(2) CO Concentration

The primary threat to people's life safety in a fire is the CO produced during the combustion process[21]. What's more, the proportion of hemoglobin(HB) in the form of carboxyhemoglobin (COHb) increases steadily as CO is inhaled causing HB to lose its ability to provide oxygen. Thus, the acute toxicity of CO depends mainly on the percentage of COHb[24]. Table 2 shows the impacts of CO concentration and exposure duration on evacuees[21].

Table 2. Effects of CO concentration and exposure duration on evacuees.

CO Concentration (ppm)	COHb (%)	Inhalation duration and symptoms of poisoning
35	<10	Headache and dizziness within 6-8h of constant exposure
100	[10,20)	Slight head ache in 2-3h
200	[20,25)	Slight headache in 2-3h; loss of judgment
400	[25,30)	Frontal headache within 1-2h
800	[30,40)	Dizziness, nausea, and convulsions within 45min; insensible within 2h
1600	[40,50)	Headache, tachycardia, dizziness, and nausea within 20min; death in less than 2h
3200	[50,60)	Headache, dizziness, and nausea in 5-10 min; death within 30 min
6400	[60,70)	Headache, dizziness, and nausea in 1-2min; convulsions, respiratory arrest, and death in less than 20min
12800	>70	Death in less than 3min

Survival is rare in subjects with blood levels exceeding 50–60% COHb and 50% COHb is usually considered as an average lethal level[24]. Thus, 1600 ppm(1.6×10^{-3}mol/mol) is considered as a threshold value.

3.5.2. External rescue environment simulation

External rescue, such as fire rescue and medical services, is necessary for all escapees[25]. Rail transit stations usually connect to the major urban roads with strong accessibility. This research investigates the route and the time required from the fire station to the complex rail transit station through the map during different periods of holidays and workdays for the evacuation assessment of the sustainable rail transit station in terms of external rescue.

Preprints (www.preprints.org) | NOT PEER-REVIEWED | Posted: 5 January 2024 doi:10.20944/preprints202401.0478.v1

4. Case study

A complex rail transit station with the underground two-floor structure was used as the study case. The selected station is located at the intersection of two rail transit lines, which presents large area, high density passenger flow, and large numbers of power lines. Thus, the station shows applicability for fire simulation and evacuation assessment. The heights of the platform floor and concourse floor are 6.05m and 5.15m, respectively. Besides, the two floors are 181.2m long and 20.7m wide. Through field investigation, the station has 37 fire-resistant doors and 9 wooden doors, which is shown in Table 3.

Table 3. Types and location of doors.

Types	Number	Size		Quantity	Location
		Width	Height		
Fire-resistant doors	FM-1	1000	2400	7	Power distribution room, control room and cable room, etc.
	FM-2	1000	2400	11	
	FM-3	1200	2700	6	
	FM-4	1200	2700	12	
	FM-5	1800	2700	1	
Wooden doors	M-1	1000	2400	7	Public works room, meeting and reception room, sewage pump room, toilet, etc.
	M-2	800	2400	2	
	M-3	1200	2700	3	

Two staircases are available for the escaping from the platform floor to the concourse floor. Besides, four exits are available for escaping from the concourse floor to the outside. The plan of the two floors of the station is shown in Figure 1.

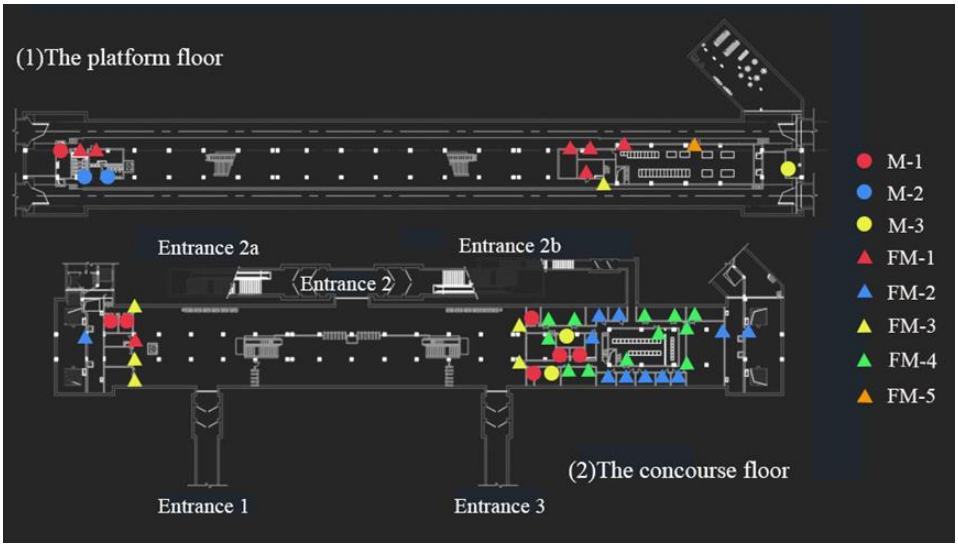

Figure 1. Plan of a complex rail transit station in Beijing.

4.1. BIM modeling and Pyrosim software

In this research, the Revit software was used for BIM modeling. The BIM model of the rail transit station case is shown in Figure 2. The operation of the Pyrosim software includes three processes: building a FDS model, conducting simulation, and analyzing simulation results. The BIM model is exported in DWG format, and then imported into the Pyrosim software to transform the BIM model into a FDS model. The temperature and CO concentration are two main monitoring parameters in FDS.

Preprints (www.preprints.org) | NOT PEER-REVIEWED | Posted: 5 January 2024 doi:10.20944/preprints202401.0478.v1

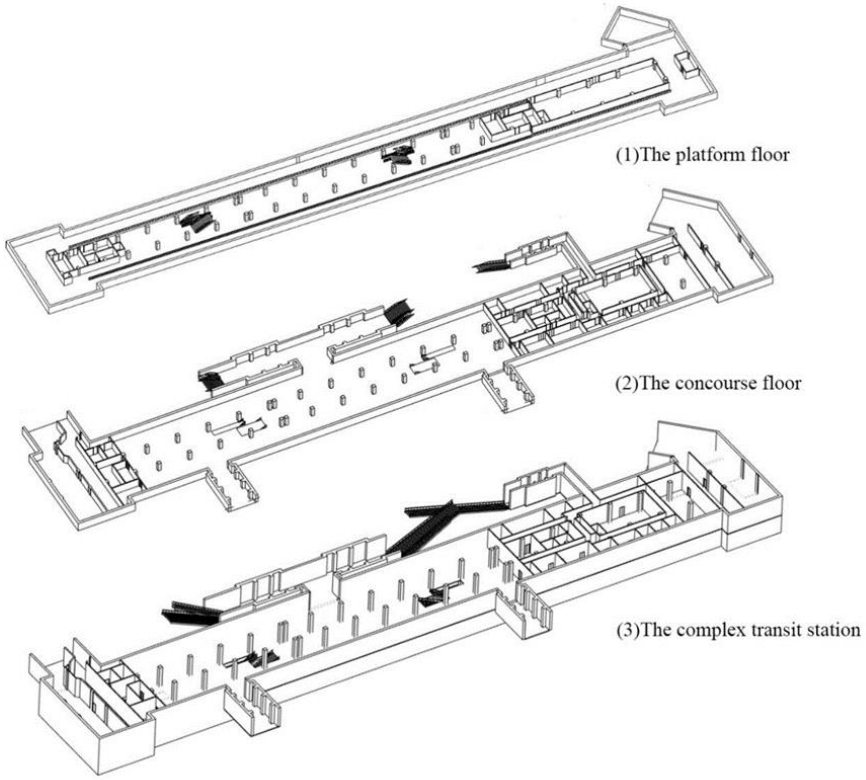

Figure 2. BIM model of the rail transit station case.

4.1.1. Combustion calculation method

In the fire simulation, the actual fire combustion process can be more closely approximated by defining the combustion reactions and setting the relevant parameters such as products of fire combustion and heat release rate. The common way to determine the pyrolysis reaction in FDS is to determine the heat release rate(HRR) on a surface[21]. In this study, the heat release rate in per unit area (HRRPUA) are specified as the combustion calculation method in Pyrosim simulation.

4.1.2. "Surfaces" parameters

The “Surface” parameters are used to define the properties of the solid objects and vents in FDS. For example, the “Burner” in the Surface parameter is used to define a fire, the “Layered” in the Surface parameter is to represent a solid and thermally conductive wall, and the “OPEN” in the Surfaces parameter is to represent a vent that is passively open to the outside and is often used to simulate an open door or window.

4.1.3. Detection equipment settings

Considering the damage of non-structural components such as fire extinguishing facilities, the locations of different fires in the complex rail transit station were determined. The detection devices include temperature detectors and CO detectors, both of which are set on the necessary escape routes, such as stairways, entrances, etc. The device numbers and locations are shown in Table 4 and Figure 3.

Preprints (www.preprints.org) | NOT PEER-REVIEWED | Posted: 5 January 2024 doi:10.20944/preprints202401.0478.v1

Table 4. Devices number and location.

The layer of the devices	Devices number	Devices	Devices location
The platform floor	1-01	(1)Temperature detector (2)CO detector	Left stairway of the platform floor
	1-02	(1)Temperature detector (2)CO detector	Right stairway of the platform floor
	1-03	(1)Temperature detector (2)CO detector	In the middle of the platform floor
The concourse floor	2-01	(1)Temperature detector (2)CO detector	Left stairway of the concourse floor
	2-02	(1)Temperature detector (2)CO detector	Right stairway of the concourse floor
	2-03	(1)Temperature detector (2)CO detector	Entrance 2
	2-04	(1)Temperature detector (2)CO detector	Entrance 1
	2-05	(1)Temperature detector (2)CO detector	Entrance 3

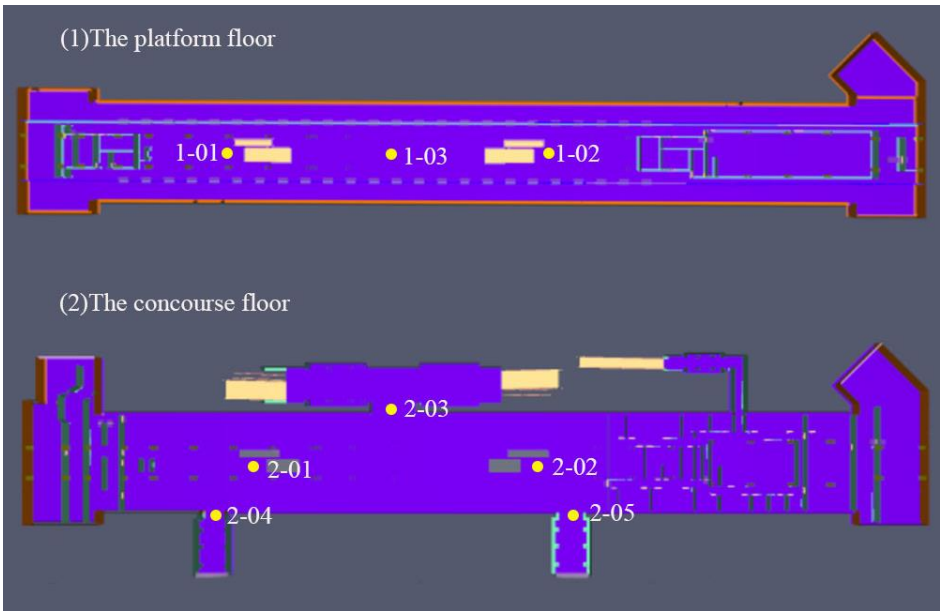

Figure 3. Plan of the detector location.

4.2. Fire scenarios

When a fire occurs in an underground station, the smoke flow usually coincides with that of the normal passenger's evacuation routes that will cause fatalities by asphyxiation[26]. In this research, two situations, the single-floor fire and the double-floor fire were considered. The six fire scenarios based on the size of the fire area are shown in Table 5.

Preprints (www.preprints.org) | NOT PEER-REVIEWED | Posted: 5 January 2024 doi:10.20944/preprints202401.0478.v1

Table 5. Fire scenarios.

Situation	Floor	Fire scenario	Fire size	Consideration
Single-floor fire (one fire point)	The platform floor	1.Large area fire in power distribution room	16.3m*5.3m	Switchgear operating equipment and transformers in the power distribution room are on the right side of the platform floor, which are prone to cause a circuit fire.
		2.Small area fire in power distribution room	5.3m*5.3m	
		3. Large area fire in the train	25.3m*3m	Assuming the train enters the station and the platform doors are all opening, while the middle of the train catches fire.
		4.Small area fire in the train	5.3m*3m	
	The concourse floor	5.Small area fire in power distribution room	5.3m*5.3m	The power distribution rooms and control rooms on the right side of the concourse floor are prone to cause fires.
Double-floor fire (two fire points)	The platform floor and The concourse floor	6.Small area fire in power distribution room on two floors	The platform floor 5.3m*5.3m The concourse floor 5.3m*5.3m	Scenario 2 and Scenario 5 occur simultaneously.

4.3. Internal evacuation environment simulation results

The time required for reaching the maximum CO concentration and the maximum temperature under the 6 fire scenarios are shown in Tables 6 and 7, respectively. The simulation diagram of temperatures under different fire scenarios is shown in Figure 4.

Table 6. The time required for reaching the maximum CO concentration.

Fire scenario	Maximum CO concentration at the platform floor (mol/mol)	The time required for the platform floor to reach the maximum CO concentration (s)	Maximum CO concentration at the concourse floor (mol/mol)	The time required for the concourse floor to reach the maximum CO concentration (s)	The fire point with the maximum CO concentration
Scenario 1	3.48E-04	175	3.89E-04	81.3	2-02
Scenario 2	2.52E-04	605	3.35E-04	598	2-02
Scenario 3	1.65E-03	288	7.18E-04	595	1-03
Scenario 4	7.17E-04	622	6.15E-05	611	1-01
Scenario 5	4.02E-06	619	2.15E-04	606	2-01
Scenario 6	2.65E-04	607	2.32E-04	614	1-03

Table 7. The time required for reaching the maximum temperature.

Fire scenario	Maximum temperature at the platform floor (℃)	The time required for the platform floor to reach the maximum temperature (s)	Maximum temperature at the concourse floor(℃)	The time required for the concourse floor to reach the maximum temperature (s)	The fire point with the maximum temperature
Scenario 1	68.1	175	84	81.3	2-03

Preprints (www.preprints.org) | NOT PEER-REVIEWED | Posted: 5 January 2024 doi:10.20944/preprints202401.0478.v1

Scenario 2	43.2	609	63.8	598	2-02
Scenario 3	418	282	65	620	1-03
Scenario 4	104	622	31.4	616	1-01
Scenario 5	20.3	567	69	605	2-01
Scenario 6	47.4	614	57.5	619	2-03

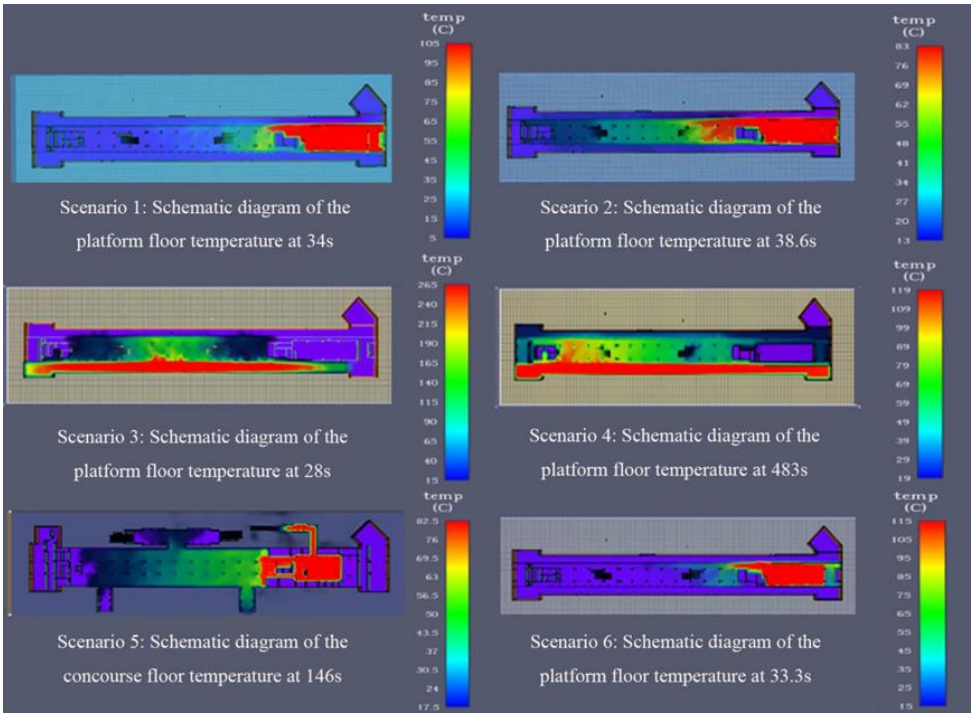

Figure 4. Simulation diagram of temperatures under different fire scenarios

4.3.1. Large area fire in power distribution room at the platform floor

In the Scenario 1, both the CO concentrations at the platform floor and the concourse floor are below the threshold values (1.6×10^{-3}mol/mol), as shown in Figure 5. The CO concentrations and temperatures of the detected points increased from the initial values and eventually fluctuated around some values. When the large area fire started in the power distribution room on the platform floor, the nearest stairway (1-02) firstly reaches the maximum CO concentration of 3.75E-05mol/mol and the maximum temperature of 30.2°C at 34s. The smoke and fire spread rapidly to the upper floor through the stairway. The gap in the stairway makes the smoke gather rapidly at the right stairway (2-02). Thus, the time of reaching the peak at the right stairway of the concourse floor is shorter than that of the platform floor. The highest CO concentration of 3.89E-04mol/mol and the highest temperature of 84°C at the concourse floor were both reached at 81.3s. Besides, the time above 60 ℃ lasted for only 3s between 81s and 83s. Then, the smoke continued to spread and reached the temperature of 68.1°C ,which lasted only 1s and the highest CO concentration is 3.48E-04mol/mol at 175s at the right stairway entrance (1-02). As shown in Table 1, the maximum exposure time is 3.8min when the exposure temperature is 80℃. The short duration of exceeding the threshold value means that the two stairway entrances (1-02) (2-02) near the distribution room have little impact on the escapees. Therefore, it is escapable for the escapees in the Scenario1.

Preprints (www.preprints.org) | NOT PEER-REVIEWED | Posted: 5 January 2024 doi:10.20944/preprints202401.0478.v1

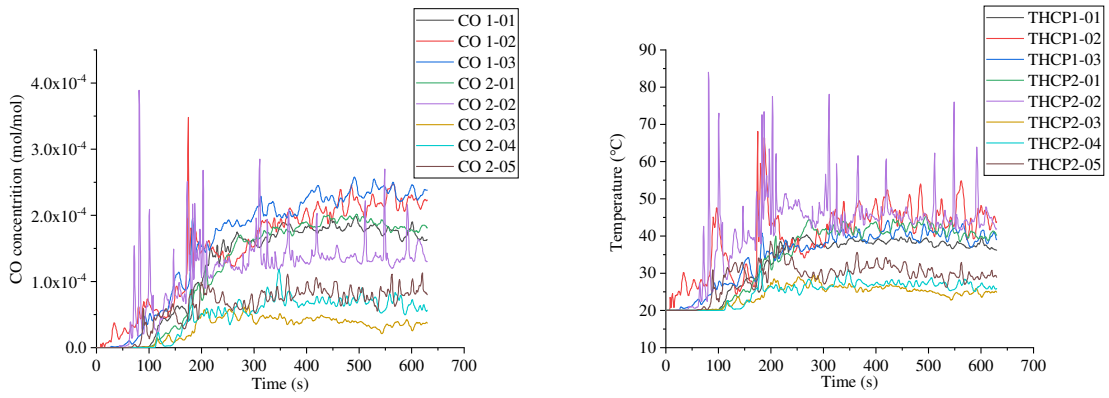

(**a**) (**b**)

Figure 5. CO concentrations and temperatures fluctuation trend under Scenario 1. (**a**) CO concentrations; (**b**) Temperatures.

4.3.2. Small area fire in power distribution room at the platform floor

In the Scenario 2, the CO concentrations and temperatures at the platform floor and concourse floor showed a gradual increase when small area fire in the power distribution room at the platform floor, as shown in Figure 6. The figures show that the CO concentrations at both the two floors did not exceed the threshold values. When the power distribution room were on fire, the nearest stairway (1-02) was the first reaching to the highest CO concentration of 6.44E-05 mol/mol and the highest temperature of 41.2℃at 38.6s. Smoke and fire spread rapidly to the upper floor through the stairway gap, resulting in the rapid accumulation of smoke at the right stairway (2-02). Therefore, the time to reach to the peak at the right stairway of the concourse floor was shorter than the platform floor. The maximum CO concentration of 3.35E-04 mol/mol at the concourse floor was reached at 595s. Later, the maximum temperature of 63.8°C at the concourse floor was reached at 598s, but only last for 2s, which is lower than the maximum human endurance time of 10.1 min. Besides, the maximum CO concentration of 3.89E-04mol/mol at the concourse floor was reached at 81.32s. With the continuous diffusion of smoke, the platform floor reached its maximum CO concentration of 2.52E-04mol/mol and the maximum temperature of 43.20°C at 609s, both of which were lower than the threshold values. Thus, it is escapable for the escapees in the Scenario 2.

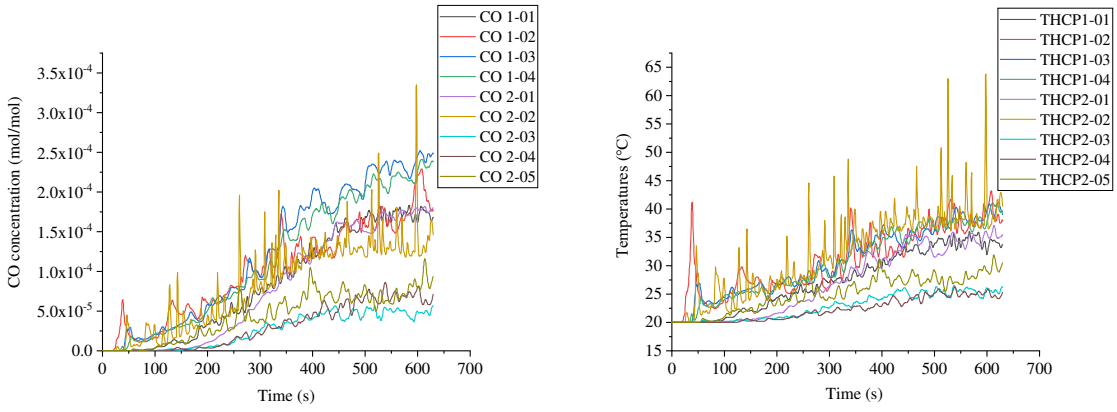

(**a**) (**b**)

Figure 6. CO concentrations and temperatures fluctuation trend under Scenario 2. (**a**) CO concentrations; (**b**) Temperatures.

4.3.3. Large area fire in the train

Large area fire in the train is considered the worst situation. As shown in Figure 7, the CO concentration and temperature of the detection points at the platform floor rapidly increased from

Preprints (www.preprints.org) | NOT PEER-REVIEWED | Posted: 5 January 2024 doi:10.20944/preprints202401.0478.v1

28s to 59s, and then gradually presented stable trend. In this scenario, CO concentration in the middle of the platform floor (1-03) has exceed 1600 ppm from 286s to 289s. Additionally, the temperature in the middle of the platform floor (1-03) has reached 60℃ at 23s, and then continued to rise over 200 ℃. Under this condition, the escape presents high difficulties. The possibility that the escapees can escape smoothly under this condition is very small.

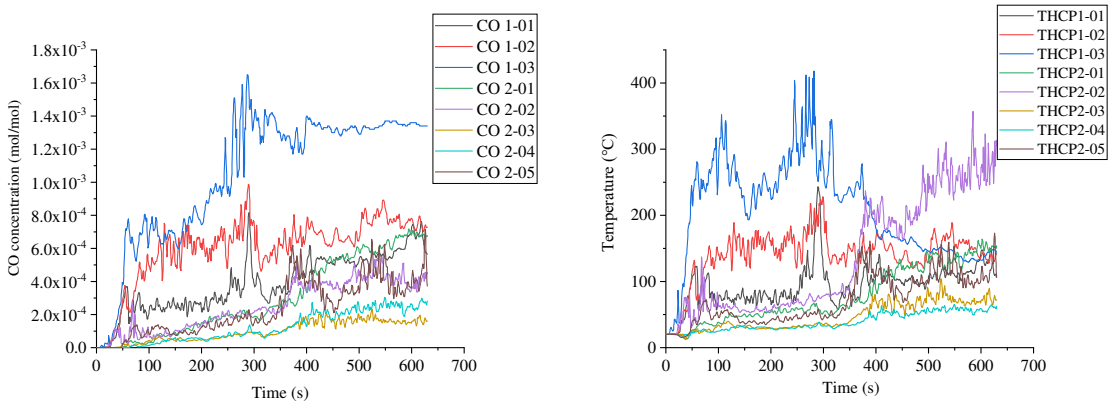

(**a**) (**b**)

Figure 7. CO concentrations and temperatures fluctuation trend under Scenario 3. (**a**) CO concentrations; (**b**) Temperatures.

4.3.4. Small area fire in the train

As shown in Figure 8, both of the CO concentration and temperature at the concourse floor increased slowly and did not exceed the threshold value. The small area fire in the train has little impact on the concourse floor. In the platform floor, the CO concentrations did not exceed the threshold value of 1600ppm. The highest CO concentration reached 7.17E-04mol/mol at 622s, and the temperature of the stairway (1-01) reached to 60°C at 330s. Subsequently, the temperature of the platform floor gradually increased and the temperatures of every detector on the platform floor reached more than 60℃ from 330s to 630s. The maximum temperature of 104 ℃ at (1-01) was reached at 622s. Thus, escaping in this situation is very difficult.

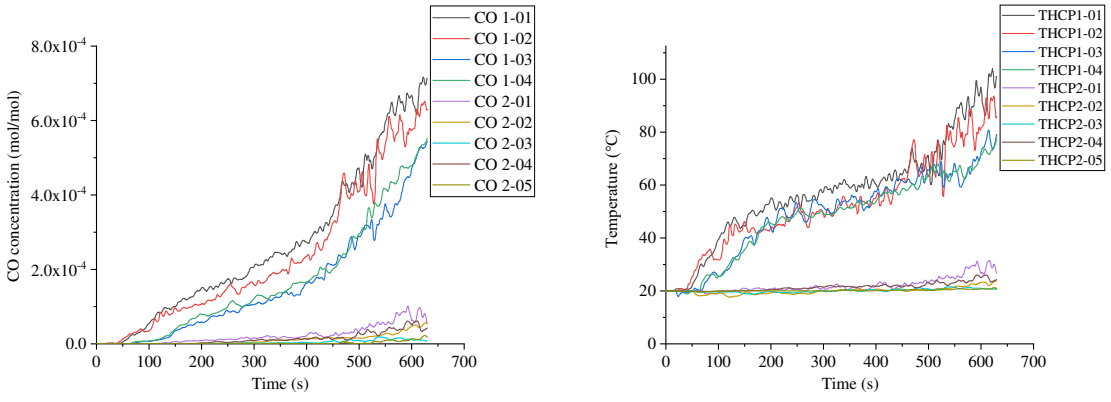

(**a**) (**b**)

Figure 8. CO concentrations and temperatures fluctuation trend under Scenario 4. (**a**) CO concentrations; (**b**) Temperatures.

4.3.5. Small area fire in power distribution room at the concourse floor

As shown in Figure 9, the CO concentration and temperature at multiple detection points at the platform floor present stable trend under Scenario 5. The fire had little impact on the platform floor ，revealing a continuous increase in CO concentration and temperature at the detection points on

Preprints (www.preprints.org) | NOT PEER-REVIEWED | Posted: 5 January 2024 doi:10.20944/preprints202401.0478.v1

the concourse floor. The concourse floor entrance nearest to the fire starting point (2-05) firstly reached to the highest temperature of 27.6°C and the highest CO concentration of 4.80E-05mol/mol at 146s. With the continuous diffusion of smoke, the stairway nearest to the fire point (2-02) reached the maximum temperature of 27.4°C and the maximum CO concentration of 4.90E-05mol/mol at 189s. Later, the stairway (2-01) (2-02) reached 60°C at the time of 597s and 594s, respectively. However, the duration that the temperature exceed 60℃ was very short, lasting only 21s for stairway (2-01) and 34s for stairway (2-02), respectively, and the maximum temperature at the concourse floor was 69℃. As shown in the Table 1, the human endurance time is 6 min when the temperature reaches 70℃. Therefore, it is escapable for the escapees in this scenario.

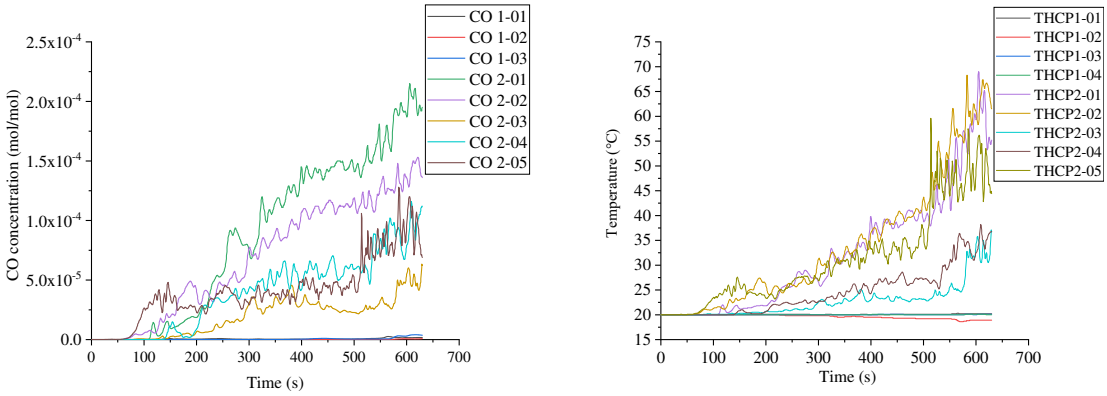

(**a**) (**b**)

Figure 9. CO concentrations and temperatures fluctuation trend under Scenario 5. (**a**) CO concentrations; (**b**) Temperatures.

4.3.6. Simultaneous small area fire in power distribution room on the two floors

As shown in Figure 10, when a small area of the power distribution room on two floors catches fire simultaneously, the CO concentration and temperature at the detection points on both floors exhibit a gradual increase over time. The stairway (1-02) nearest to the power distribution room on platform floor reached the highest temperature of 32.9°C and the highest CO concentration of 9.85E-05mol/mol at 33.3s. With the continuous diffusion of smoke, the middle position of the platform floor (1-03) reached the maximum temperature of 24°C and the maximum CO concentration of 1.34E-05mol/mol at 69.3s. The nearest entrance to the fire starting location (2-05) reached the maximum temperature of 38°C and the maximum CO concentration of 1.39E-04mol/mol at 199s. Besides, the maximum CO concentration of 2.65E-04mol/mol at the platform floor was reached at 607s, and the maximum temperature of 47.4°C at the platform floor was reached at 614s. Additionally, the maximum CO concentration of 2.32E-04mol/mol at the concourse floor was reached at 614s, and the maximum temperature of 57.5℃ at the concourse floor was reached at 619s. It has been confirmed that both the maximum CO concentration and the maximum temperature were lower than the threshold value. Thus, it is safe to escape in this scenario.

Preprints (www.preprints.org) | NOT PEER-REVIEWED | Posted: 5 January 2024 doi:10.20944/preprints202401.0478.v1

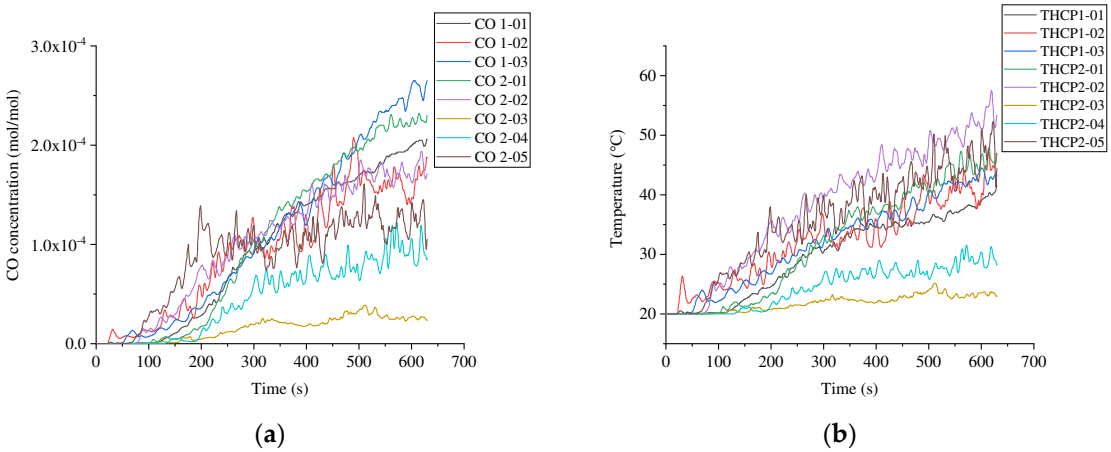

(**a**) (**b**)

Figure 10. CO concentrations and temperatures fluctuation trend under Scenario 6. (**a**) CO concentrations; (**b**) Temperatures.

In summary, it becomes difficult to escape when large area fire or small area fire occurs in the train, which are Scenario 3 and Scenario 4. Comparatively, it is possible to escape in the Scenario 1, Scenario 2, Scenario 5 and Scenario 6 when the fire occurs in the power distribution room.

4.4. External rescue environment simulation results

Through investigating the surrounding environment, two fire stations are 6.2km and 4.2km away from the complex rail transit station, as shown in Figure 11. The road condition from fire station A and fire station B to the complex rail transit station are observed though electronic map in all time of a day from "0:00" to "24:00". It was found that the roads were consistently smooth on both workdays and holidays. Thus, the fire engine can smoothly travel from fire station A and fire station B to the complex rail transit station.

(**a**) (**b**)

Figure 11. Routes from two fire stations to the complex rail transit station. (**a**) Route from fire station A to the station; (**b**) Route from fire station B to the station.

In China, the planning and construction of urban fire stations are regulated by the Code for Planning of Urban Fire Control GB 51080-2015 and Construction Standards for Urban Fire Station 152-2017. The Construction Standards for Urban Fire Station 152-2017 indicates that the rescuers should arrive at the fire scene within 5min after receiving the dispatch command. It is assumed that no surrounding collapsed houses and no traffic congestion on the roads after the earthquake. According to the real-time road condition analysis by the electronic map, a fire vehicle takes approximately 4min and 3min to reach the complex rail transit station from the fire station A and the fire station B, respectively. However, uncertainties such as weather and road conditions may arise during the firefighting vehicles moving from the fire station to the complex rail transit station. Due to the potential for damage to surrounding buildings, blocked access, and additional rescue tasks that fire stations must attend to after an earthquake, ensuring timely rescue is a considerable challenge.

Preprints (www.preprints.org) | NOT PEER-REVIEWED | Posted: 5 January 2024 doi:10.20944/preprints202401.0478.v1

5. Discussion

5.1. The influence of different fire areas

According to Section 3.3, the assessment results indicate that evacuation is feasible when a fire occurs in the power distribution room. However, evacuating becomes challenging when a fire breaks out on the platform floor of a train. Scenario 1, Scenario 2, Scenario 3, and Scenario 4 were selected for analyzing the influence of different fire areas on CO concentration and temperature. The stairway (1-02) nearest to the power distribution room on platform floor in Scenario 1 and Scenario 2 and the middle position of the platform floor (1-03) in Scenario 3 and Scenario 4 are considered for the analysis. The results of the CO concentrations and temperatures fluctuation trend are shown in Figures 12 and 13. The difference of temperature and CO concentration in Scenario 1 and Scenario 2 are smaller than those in Scenario 3 and Scenario 4. Taking the example of 300s, in Figure 12, the CO concentration is 1.53E-04mol/mol and the temperature is 37.3 ℃ under a large area fire, while under the small area fire is 9.3E-05mol/mol and 26.2℃, respectively. As shown in Figure 13, the CO concentration is 7.59E-04mol/mol and the temperature is 225 ℃ under the large area fire, while the CO concentration is 1.59E-04mol/mol and the temperature is 48.7 ℃ under a small area fire. In this case, there is a difference of 6E-04mol/mol in CO concentration and 176.3℃ in temperature between the large area fire and the small area fire.

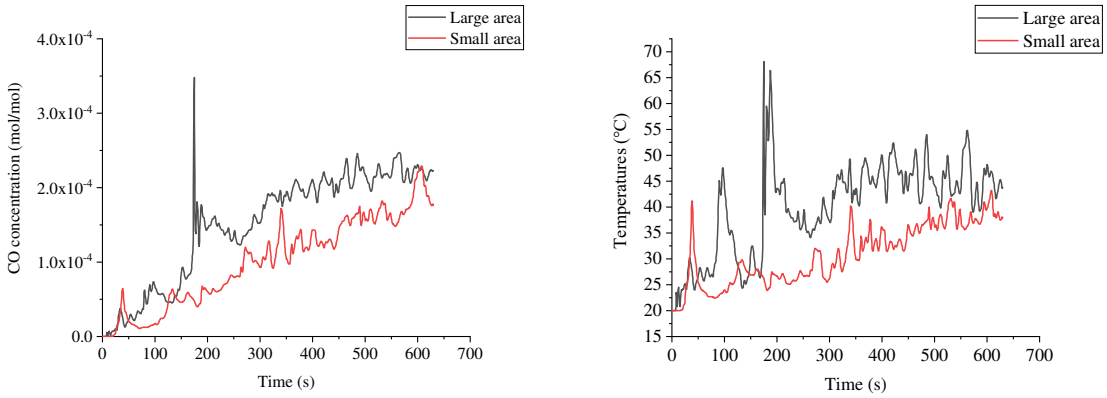

(**a**) (**b**)

Figure 12. CO concentrations and temperatures fluctuation trend of (1-02) under Scenario 1 and Scenario 2. (**a**) CO concentrations; (**b**) Temperatures.

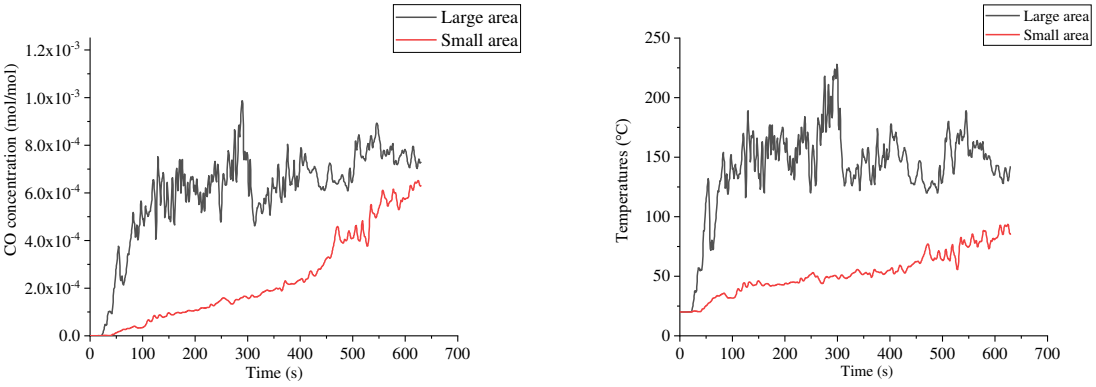

(**a**) (**b**)

Figure 13. CO concentrations and temperatures fluctuation trend of (1-03) under Scenario 3 and Scenario 4. (**a**) CO concentrations; (**b**) Temperatures.

It can be seen that the CO concentration and temperature generated by large area fires are generally higher than those of small area fires. Besides, the influence caused by different size of the

Preprints (www.preprints.org) | NOT PEER-REVIEWED | Posted: 5 January 2024 doi:10.20944/preprints202401.0478.v1

post-earthquake fire area in the power distribution room at the platform floor is smaller than those in the train at the platform floor. For a fire in the power distribution room, smoke can only flow through open doors, while for a fire in the train, smoke could enter the open space through all doors on the train.

5.2. The influence of different fire locations

In Scenario 2 and Scenario 5, although the fire areas are the same, the fire locations differ. In these two scenarios, the stairways nearest to the fire point (1-02) and (2-02) are chosen for analyzing. As shown in Figure 14, the CO concentration in (2-02) is lower than that in (1-02), and the difference in CO concentration between the two scenarios is 0.4E-04mol/mol at 630s. As for temperature, the temperature in (1-02) is initially higher than that in (2-02), but the temperature increase rate in (2-02) is significantly greater than that in (1-02). Subsequently, the temperature becomes consistent at 177s, and the final temperature in (2-02) is 23.6℃ higher than that in (1-02).

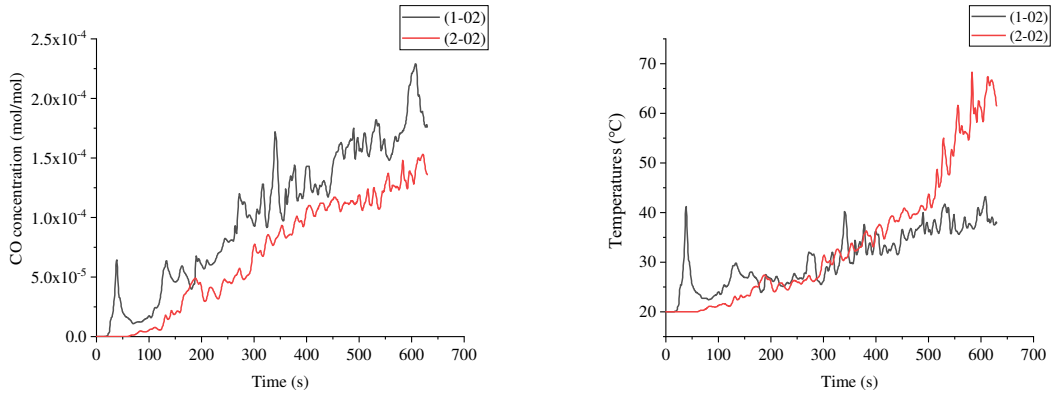

(**a**) (**b**)

Figure 14. CO concentrations and temperatures fluctuation trend of (1-03) under Scenario 2 and Scenario 5. (**a**) CO concentrations; (**b**) Temperatures.

According to the results, the CO concentration presents consistent fluctuation trend for the small area fire in power distribution room in different floors of the station, while the temperature fluctuation show more obvious differences.

5.3. The influence of single-floor fire and double-floor fire

To compare the different impact of single-floor fire and double-floor fire on evacuation, Scenario 2, Scenario 5, and Scenario 6 were selected with the same fire area for analysis. In this paper, (1-02) was selected as the analysis area to explore the difference between single-floor fire in Scenarios 2 and double-floor fire in Scenario 6. Besides, (2-02) was selected as the analysis area for Scenario 5 and Scenario 6.

The analysis results are shown in Figure 15. Regarding CO concentration, the increase rate in Scenario 2 and Scenario 6 is relatively consistent. At 630s, the difference in CO concentration between the two scenarios is only 0.11E-04mol/mol. Regarding temperature, the temperatures show gradually increasing trend, and the temperature becomes consistent at 602 s. At 630s, the temperature difference between Scenario 2 and Scenario 6 is only 9℃. As shown in Figure 16, the CO concentrations in the two scenarios become the same at 83s. Subsequently, the CO concentration in Scenario 6 is generally higher than that in Scenario 5. Finally, the CO concentration difference between Scenario 5 and Scenario 6 is 0.35E-4mol/mol at 630s. Besides, the temperature in Scenario 6 is initially higher than that in Scenario 5, but the temperature increase in Scenario 5 is faster than that in Scenario 6. The temperatures become consistent at 542s, and at 630s, the temperature in Scenario 5 is 8.1℃ higher than that in Scenario 6.

Preprints (www.preprints.org) | NOT PEER-REVIEWED | Posted: 5 January 2024 doi:10.20944/preprints202401.0478.v1

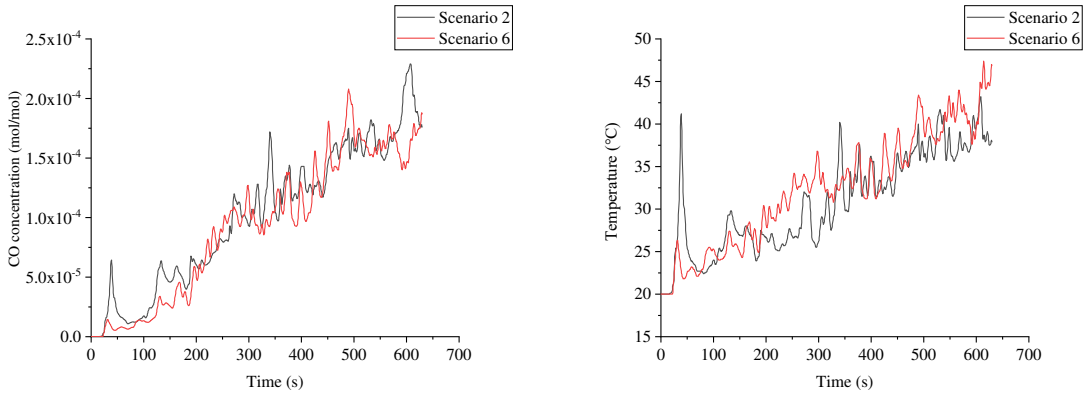

(**a**) (**b**)

Figure 15. CO concentrations and temperatures fluctuation trend of (1-02) under Scenario 2 and Scenario 6. (**a**) CO concentrations; (**b**) Temperatures.

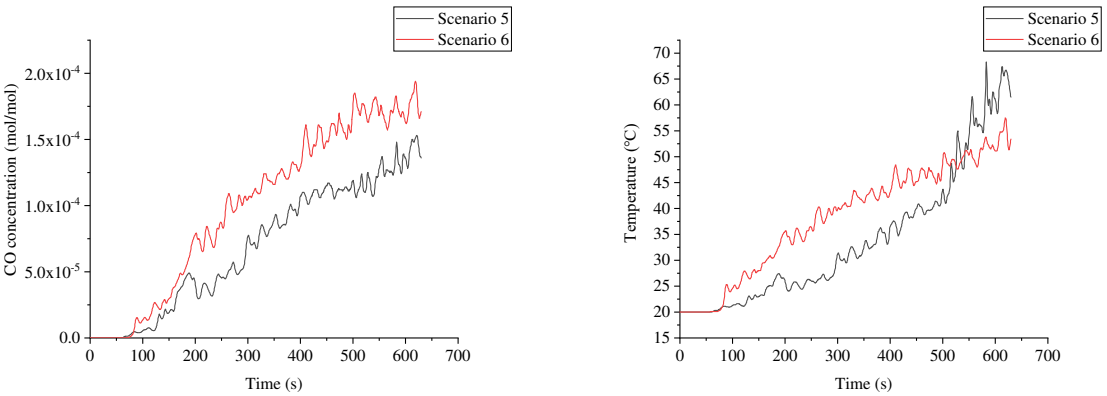

(**a**) (**b**)

Figure 16. CO concentrations and temperatures fluctuation trend of (2-02) under Scenario 5 and Scenario 6. (**a**) CO concentrations; (**b**) Temperatures.

According to the above results, it shows slight differences of the influence on evacuation for small area fire in power distribution room on single-floor or double-floor.

6. Conclusion

Post-earthquake fires have a significant impact on personal and property safety. This paper conducts an evacuation assessment of complex rail transit station under post-earthquake fires for sustainable buildings based on BIM and FDS. It is assumed that the building structures have no visible damage and the escape routes are not disrupted in the initial minutes of the fire after the earthquake. By establishing a fire simulation model based on BIM and FDS, this paper assess the feasibility of evacuation in a complex rail transit station under post-earthquake fires through monitoring temperature and CO concentration. Besides, this paper considers external factors related to disaster relief to determine whether external rescue forces can promptly arrive at the complex rail transit station to provide rescue coverage.

According to the research results, optimized design recommendations are proposed for reducing the risk of emergency evacuation in both internal and external environments of rail transit stations to achieve sustainable buildings.

(1) The power distribution room in the complex rail transit station should be designed away from the public areas, such as stairs, or it can be set in a relatively independent area. Setting the power distribution room on the concourse floor is recommended.

(2) In addition to fire-resistant doors, installing fireproof curtains or shutters around the power distribution rooms is recommended to minimize the spread of fire and smoke.

(3) To improve the safety of complex rail transit stations, it is essential to increase the quantity of smoke detectors and alarms, particularly in high-risk areas like power distribution rooms and trains. Regular maintenance and testing should also be concluded to ensure their effectiveness.

(4) The influence of a large area fire has a greater impact on evaluation assessment than that of a small area fire. Thus, the area of the power distribution room should be as small as possible when available, and fire-resistant doors should be installed to mitigate the effects of the fire.

(5) The research shows that the influence of a fire in train is more serious than that of a fire in power distribution room. Therefore, it is crucial to develop specific emergency plans for train fires to address this issue effectively.

(6) In urban planning, more small fire stations should be planned around complex public buildings such as complex rail transit stations to avoid road obstruction difficulties after an earthquake.

Besides, this study did not consider the possibility of confusion during the evacuation after an earthquake, such as crowded situation. The chaotic situations might prevent a safe evacuation. Developing reasonable passenger escape route plans under a post-earthquake fire in the complex rail transit stations should be considered as a future research direction.

Author Contributions: Conceptualization, H.X. , Y.W. and Q.Z.; methodology, H.X. ,Y.W. and Y.T.; software, H.X. and Y.W.; validation, H.X. and Y.W.; formal analysis, H.X. , Y.W. and Q.Z.; investigation, H.X. , Y.W. and Q.Z.; resources, H.X. , Y.W. and Y.T.; data curation, H.X. and Y.W.; writing—original draft preparation, H.X. ,Y.W., Q.Z. and Y.T.; writing—review and editing, H.X. , Y.W., Q.Z. and Y.T.; visualization, H.X. and Y.W.; supervision, H.X.; project administration, H.X.; funding acquisition, H.X. All authors have read and agreed to the published version of the manuscript.

Funding: This research was funded by The General Project of Chongqing Natural Science Foundation (Grant No. cstc2021jcyj-msxmX0951); The Western Project of the National Social Science Fund of China (Grant No. 22XGL013); The China Postdoctoral Science Foundation (Grant No. 2021M700617); The Innovative Project of Chongqing Oversea Study Innovation Program (Grant No. cx2020035).

Data Availability Statement: The data presented in this research are available upon request from the corresponding author. The data are not publicly available due to privacy.

Conflicts of Interest: No potential conflict of interest was reported by the authors.

References

1. Lou, T.; Wang, W.; Li, J. Post-earthquake fire behaviour of a self-centring connection with buckling-restrained plates and pre-stressed bars: An experimental investigation. *J. Build. Eng.* **2022**,*56*,104733. doi: 10.1016/j.jobe.2022.104733.
2. Historical query of China Earthquake Networks Center. China Earthquake Networks Center. Available online: http://www.ceic.ac.cn/history. (accessed on 24 Nov 2023).
3. Ni, S.; Birely, A.C. A simplified model for the post-fire earthquake flexural response of reinforced concrete walls with boundary elements. *Eng. Struct.* **2018**,*175*,721-730. doi: 10.1016/j.engstruct.2018.08.044.
4. Risco, G.V.; Zania, V.; Giuliani, L. Numerical assessment of post-earthquake fire response of steel buildings. *Saf. Sci.* **2023**,*157*,105921. doi: 10.1016/j.ssci.2022.105921.
5. Trifunac, M.D.; Todorovska, M.I. The Northridge, California, earthquake of 1994: fire ignition by strong shaking. *Soil Dyn. Earthquake Eng.* **1998**,*17*,165–175. doi: 10.1016/S0267-7261(97)00040-7.
6. Nishino, T. Probabilistic analysis of the vulnerability of fire departments to ignitions following megathrust earthquakes in the Nankai Trough subduction zone, Japan. *Fire Saf. J.* **2021**,*120*,103038. doi: 10.1016/j.firesaf.2020.103038.
7. Xu, H.; Li, Y.; Wang, L. Resilience Assessment of Complex Urban Public Spaces. *Int. J. Environ. Res. Public Health* **2020**,*17(2)*,524. doi: 10.3390/ijerph17020524.
8. Li, M.; Wang, Y.H.; Jia, L.M. On operation safety assessment model for urban rail transit station. *Adv. Transp. Stud.* **2015**,*1*,13-22. doi: 10.4399/978885488881402.

9. Xu, H.; Xue, B. Key indicators for the resilience of complex urban public spaces. *J. Build. Eng.* **2017**,*12*,306-313. doi: 10.1016/j.jobe.2017.06.018.
10. Zhang, J.; Chen, T.; Su, G.; Li, C.; Zhao, F.; Mi, F. Microstructure and component analysis of glowing contacts in electrical fire investigation. *Eng. Fail. Anal.* **2022**,*140*, 106539. doi: 10.1016/j.engfailanal.2022.106539.
11. Sarreshtehdari, A.; Khorasani, N.E. Integrating the fire department response within a fire following earthquake framework for application in urban areas. *Fire Saf. J.* **2021**,*124*, 103397. doi: 10.1016/j.firesaf.2021.103397.
12. Feng, J.; Gai, W.; Yan, Y. Emergency evacuation risk assessment and mitigation strategy for a toxic gas leak in an underground space: The case of a subway station in Guangzhou, China. *Saf. Sci.* **2021**,*134*, 105039. doi: 10.1016/j.ssci.2020.105039.
13. Chen, Y.; Wang, C.; Yap, J.B.H.; Li, H.; Zhang, S. Emergency evacuation simulation at starting connection of cross-sea bridge: Case study on Haicang Avenue Subway Station in Xiamen Rail Transit Line. *J. Build. Eng.* **2020**, *29*, 101163. doi: 10.1016/j.jobe.2019.101163.
14. Xu, H.; Tian, C.; Li, Y. Emergency Evacuation Simulation and Optimization for a Complex Rail Transit Station: A Perspective of Promoting Transportation Safety. *J. Adv. Transp.* **2020**,*2020*,1-12. doi: 10.1155/2020/8791503.
15. Juliá, P.B.; Ferreira, T.M.; Rodrigues, H. Post-earthquake fire risk assessment of historic urban areas: A scenariobased analysis applied to the Historic City Centre of Leiria, Portugal. *Int. J. Disaster Risk Reduct.* **2021**,*60*,102287. doi:10.1016/j.ijdrr.2021.102287.
16. Lu, X.; Yang, Z.; Xu, Z.; Xiong, C. Scenario simulation of indoor post-earthquake fire rescue based on building information model and virtual reality. *Adv. Eng. Software* **2020**,*143*, 102792. doi: 10.1016/j.advengsoft.2020.102792.
17. Xu, Z.; Zhang, Z.; Lu, X.; Zeng, X.; Guan, H. Post-earthquake fire simulation considering overall seismic damage of sprinkler systems based on BIM and FEMA P-58. *Autom. Constr.* **2018**,*90*,9-22. doi: 10.1016/j.autcon.2018.02.015.
18. Zhang, W.; Liu, Y.; Yu, S.; Zhang, Y.; Yang, L.; Qi, L. The Application Research of BIM Technology in the Construction Process of Yancheng Nanyang Airport. *Buildings* **2023**, *13(11)*, 2846. doi: 10.3390/buildings13112846.
19. Deng, H.; Wei, X.; Deng, Y.; Pan, H.; Deng, Q. Can information sharing among evacuees improve indoor emergency evacuation? An exploration study based on BIM and agent-based simulation. *J. Build. Eng.* **2022**,*62*,105418. doi: 10.1016/j.jobe.2022.105418.
20. Xu, L.; Huang, K.; Liu, J.; Li, D.; Chen, Y.F. Intelligent planning of fire evacuation routes using an improved ant colony optimization algorithm. *J. Build. Eng.* **2022**,*61*,105208. doi: 10.1016/j.jobe.2022.105208.
21. Lotfi, N.; Behnam, B.; Peyman, F. A BIM-based framework for evacuation assessment of high-rise buildings under post-earthquake fires. *J. Build. Eng.* **2021**,*43*,102559. doi: 10.1016/j.jobe.2021.102559.
22. *Report on the Nutrition and Chronic Disease Status of Chinese Residents*; The State Council Information Office of the People's Republic of China: China,2022.
23. *NFPA130:Standard for the Fixed Guideway Transit and Passenger Rail Systems*; National Fire Protection Association: America,2020.
24. Purser, D.A.; McAllister, J.L. Assessment of Hazards to Occupants from Smoke, Toxic Gases, and Heat; In *SFPE Handbook of Fire Protection Engineering*, 5th ed.; Springer: New York, 2016; pp. 2308-2428.
25. Hahne, D.; Rehm, S. Full-scale tests of external rescue with firefighters in underground stations. *Fire Saf. J.* **2022**,*128*, 103538. doi.org/10.1016/j.firesaf.2022.103538.
26. Yang, H.; Li, S. Numerical Investigation on the Effect of Mobile Smoke Ventilator on Fire-induced Smoke Extraction for Underground Platform in a High-speed Railway Station. *Procedia Eng.* **2018**,*211*,871–880. doi: 10.1016/j.proeng.2017.12.086.